FUNDAMENTAL STUDY OF BUBBLE DISSOLUTION IN LIQUID

Y. MORI, K. HIJIKATA and T. NAGATANI

Department of Physical Engineering, Tokyo Institute of Technology, Ohokayama 2,
Meguro-ku, Tokyo 152, Japan

Abstract—As a fundamental step for the study of extinction and generation of bubble nucleas in boiling and cavitation, a theoretical and experimental study was made on extinction behaviors of gas bubble by making use of the droplet system containing gas bubble. The small gas bubble in the droplet, whose diameter decreases with the rise of pressure, is found to extinguish when it reaches a certain critical pressure at a certain finite bubble diameter. The phenomenon is analysed from a thermodynamical instability by considering the dissolution of gas into liquid. It is made clear that there holds a fairly good agreement between the theoretical prediction and experimental results with regard to the critical pressure and bubble radius.

NOMENCLATURE

A, area $[m^2]$;
K, solubility coefficient $[m^2/N]$;
F, free energy $[J]$;
n, mole number;
p, pressure $[Pa, atm]$;
r, radius of ball $[m]$;
R, gas constant of 1 mol $[J/mol\,K]$;
T, temperature $[K]$;
V, volume $[m^3]$;
v, volume per unit mole $[m^3/mol]$;
x, mole fraction;
k, compression coefficient of liquid $[m^2/N]$.

Greek symbols

σ, surface tension $[N/m]$;
μ, chemical potential $[J/mol]$;
μ^0, standard chemical potential $[J/mol]$.

Superscripts and subscripts

1, liquid component of droplet;
2, component of noncondensable gas;
$'$, gas phase;
$''$, liquid phase of droplet;
$'''$, liquid phase of surrounding medium;
σ, gas–liquid interface;
gL, liquid–liquid interface;
e, status at extinction of bubble.

1. INTRODUCTION

BOILING and cavitation are the most important phenomena in heat transfer. The study of formation of initial bubble is considered especially important in clarifying the minimum limit of boiling heat transfer. A number of discussions have been made on effect of noncondensable gas extended on phase change from liquid to gas. However, it has not been made clear in what mechanism the noncondensable gas gives effect on phase change such as boiling. In the study of cavitation, only the effect of noncondensable gas has been taken up, its parameter being an air content, and no experimental

method to clarify the mechanism has been established. On the other hand, in the study of boiling it may be very difficult to make a quantitative experimental study on existence of gas bubble kept in the small cavity on the boiling surface. Therefore, to investigate such a weak behavior of gas bubble in the liquid phase, an experiment has to be carried out under such condition that its theoretical analysis can be made and it is also necessary to observe the bubble clearly. Furthermore, it is desired to clarify what effect may be extended to this phase transfer by the gas completely dissolved.

Wakeshima *et al.* [1] have reported that on homogeneous nucleation in the liquid with no cause of nuclear generation such as a small solid body, ion and cosmic rays. They showed that when the liquid is of a single component the superheat limit of liquid agrees with the theoretical result of Döring [2], under the experiment by using the floating droplet method. Skripov [3] made various experiments on hydrocarbons and showed an agreement between the theory and the experiment. Later, Döring's theory has been theoretically developed [4] and recently results of study [5, 6] on homogeneous nucleation in connection with thermal explosion at accident of liquid natural gas system, nuclear reactor, etc., have been reported.

It is considered that the gas bubble in the liquid plays an important role for homogeneous nucleation, and, therefore, in the present report a theoretical analysis and experimental result are reported. The stress is made on behaviors of small gas bubble in the droplet and stability of existence of bubble as a fundamental step to study effect of noncondensable gas extended to the phase changes of liquid–gas of boiling, cavitation and such.

2. EXPERIMENTAL APPARATUS AND METHOD

As shown in Fig. 1, in a sufficient volume of liquid a small droplet of other liquid floating unsoluble is made, and furthermore, a small bubble containing noncondensable gas is included in this droplet. By making use of this droplet system, behaviors of the bubble are
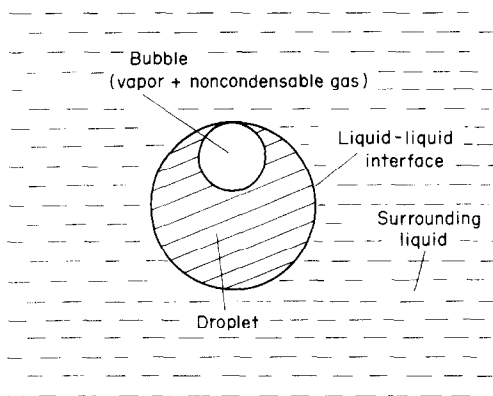
41

FIG. 1. Physical model.

observed through a microscope to investigate the possibility of existence of this bubble and to measure the volume of gas dissolved in this droplet. Glycerine was adopted as the surrounding liquid, freon 21 as the liquid of droplet.

In Fig. 2, a whole diagram of experimental apparatus is shown. It is made up of the following three sections: The mixing section makes a mixture gas consisting of a small amount of noncondensable gas and freon 21 vapor, in the test section a droplet is made and observed, and, finally, the damp tank is to control pressure in the test section.
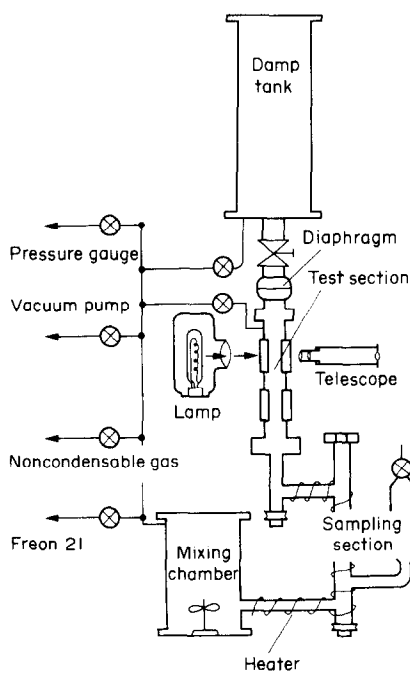

FIG. 2. Experimental apparatus.

To change the pressure of the test section, the breaking of film set between the tank and test section was done and a needle valve was used to control the pressure of test section gradually by about every 0.01 atm. In Fig. 3, the detail of the test section, where glycerine is filled, is shown. A bubble of mixture gas of 2–3 mm dia was sent into glycerine from the glass nozzle at the lower part of the test section. The mixture gas consisted of freon 21 and other noncondensable gases
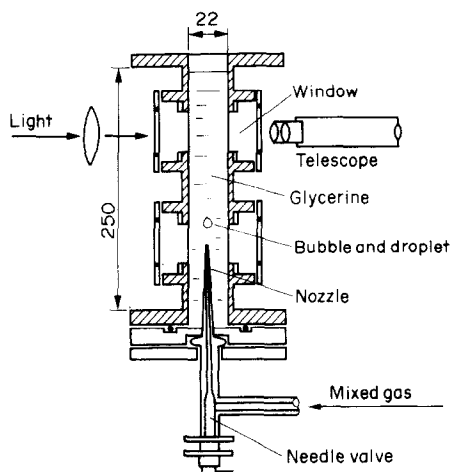

FIG. 3. Details of test section.

such as N_2, O_2, CO_2, which was so mixed as to be uniformly composed, and its component was accurately measured just before the experiment. Before this bubble arrived at the observation window at the upper part of the test section, the pressure in the test section was gradually increased beyond the saturation pressure of freon 21, and the vapor of freon 21 in the bubble was made condensed. Thus the bubble of 2–3 mm dia became a small droplet containing a bubble of about 0.2 mm dia, mostly consisting of noncondensable gas, and it rose up in glycerine. When this droplet containing a bubble arrived at the observation window, it was lighted so that the shape could be observed clearly. At this position a telescopic microscope of magnification of 70 times was focused and was traversed up and down.

An example of the experimental results obtained from microscopic observation of bubble and pressure measurement is shown in Fig. 4. This shows the relation between the pressure p and the bubble radius r. For example, at the pressure 3.134 atm the droplet of 150μ in radius contains a bubble of 87.0μ in radius. When the pressure is slowly raised so as to be isothermally changed, the radius of the bubble decreases, and at the
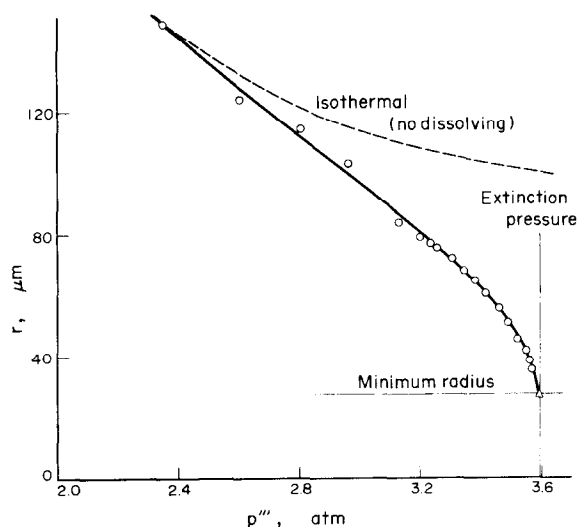

FIG. 4. Relation between pressure and bubble radius.

pressure 3.59 atm, shown with a broken line in the figure, the bubble suddenly extinguishes. The isothermal p–r relation, which assumes no dissolving gas into the liquid phase, is shown with a broken line in Fig. 4. According to the experiment, with the increase of pressure the bubble radius becomes smaller than the values assumed by isothermal change and it is known that the gas is dissolved in the liquid phase.

3. THEORETICAL ANALYSIS

In order to examine theoretically the behaviors of bubble contained in the droplet system that are experimentally shown in the foregoing section, a thermodynamic equilibrium condition of two component two phase system consisting of droplet and bubble, shown in Fig. 1, is introduced, and the thermodynamic stability of its equilibrium point is discussed. The droplet containing a bubble is assumed to be floating in the surrounding liquid of a sufficiently large volume. When a liquid of very large viscosity is assumed for the surrounding liquid, the droplet containing a small gas bubble is regarded to stand still in this liquid for a short time. In this case, the reason for using the surrounding liquid is to make the observation of the droplet and the bubble and for the gas to be dissolved homogeneously in the droplet of finite volume. This makes it easy to compare the experiment and the theory. However, by making the radius of the droplet infinite, the result of the present investigation is applicable to discussion of behaviors of bubbles in infinite liquid.

The following assumptions are made on analysis:

(1) The noncondensable gas in the droplet is assumed not to diffuse outside through the boundary surface of the droplet system.

(2) The droplet system is assumed to be isothermal.

(3) The liquid and gas phase of the droplet system are of the ideal system of activity coefficient 1.

(4) The volume of the liquid phase in the droplet system is constant.

(5) The droplet and the gas bubble in the droplet are of spherical shape.

When the surface tension acting on the liquid–liquid interface is considerably larger than the surface tension of the liquid gas interface of bubble, the bubble and the droplet mostly keep spherical shapes [7]. Therefore, when the above mentioned conditions are satisfied, assumption (5) is appropriate. Practical combinations of liquid satisfying the assumptions stated above should be investigated. As one example of surrounding liquid, glycerine, a liquid of high viscosity and of strong polarity, can be adopted. As for liquid of droplet, hydrocarbons of low boiling point such as hexane, pentane, ether, etc., and halogen compounds such as R-21, R-114, R-113, etc., can be adopted.

δF, the change of free energy of the droplet system that contains bubble, is equal to the work received from outside, and if the pressure of surrounding liquid is assumed p''', the following equation is obtained.

$$\delta F + p''' \delta V_{gL} = 0 \qquad (1)$$

here

$$\delta \mathbf{F} = \delta F + p''' \delta V_{gL} \qquad (2)$$

is introduced. As seen from Fig. 1, the droplet system containing a bubble consists of liquid phase (droplet), gas phase (bubble), gas–liquid interface, and liquid–liquid interfaces. Therefore, the change of free energy of the system is equal to the sum of changes of free energy of respective phases.

$$\delta F = \delta F' + \delta F'' + \delta F^\sigma + \delta F^{gL} \qquad (3)$$

where ' indicates the gas phase, " the liquid phase of droplet, ''' that of the surrounding liquid, σ the gas liquid interface, and gL the liquid–liquid interface. By using assumptions (2) and (4), changes of free energy of the respective phases can be given as follows:

$$\delta F' = \left(\frac{\partial F'}{\partial V'}\right)_{n_1 n_2} \delta V' + \left(\frac{\partial F'}{\partial n_1'}\right)_{V' n_2'} \delta n_1' + \left(\frac{\partial F'}{\partial n_2'}\right)_{V' n_1'} \delta n_2'$$
$$= -p' \delta V' + \mu_1'(T, p_1') \delta n_1' + \mu_2'(T, p_2') \delta n_2' \qquad (4)$$

$$\delta F'' = \left(\frac{\partial F''}{\partial n_1''}\right)_{n_2'} \delta n_1'' + \left(\frac{\partial F''}{\partial n_2''}\right)_{n_1'} \delta n_2''$$
$$= \mu_1''(T, p'', x_1'') \delta n_1'' + \mu_2''(T, p'', x_2'') \delta n_2'' \qquad (5)$$

$$\delta F^\sigma = \sigma \delta A = \frac{2\sigma}{r} \delta V' \qquad (6)$$

$$\delta F^{gL} = \sigma_{gL} \delta A_{gL} = \frac{2\sigma_{gL}}{r_{gL}} \delta V_{gL} \qquad (7)$$

where, μ is a chemical potential, and n is a mole number. We also have

$$V_{gL} = V' + V'', \quad V'' = \text{const.}, \quad \delta V_{gL} = \delta V' \qquad (8)$$

$$n_1' + n_1'' = n_{10}, \quad n_{10} = \text{const.}, \quad \delta n_1' = -\delta n_1'' \qquad (9)$$

$$n_2' + n_2'' = n_{20}, \quad n_{20} = \text{const.}, \quad \delta n_2' = -\delta n_2''. \qquad (10)$$

Considering the above mentioned equations, and using equations (3)–(7), we have

$$\delta \mathbf{F} = \left(-p' + p''' + \frac{2\sigma}{r} + \frac{2\sigma_{gL}}{r_{gL}}\right) \delta V' + \{\mu_1'(T, p_1')$$
$$- \mu_1''(T, p'', x_1'')\} \delta n_1' + \{\mu_2'(T, p_2')$$
$$- \mu_2''(T, p'', x_2'')\} \delta n_2' \qquad (11)$$

and, consequently, the following equations are obtained as equilibrium condition.

$$p' - p''' = \frac{2\sigma}{r} + \frac{2\sigma_{gL}}{r_{gL}} \qquad (12)$$

$$\mu_1'(T, p_1') = \mu_1''(T, p'', x_1'') \qquad (13)$$

$$\mu_2'(T, p_2') = \mu_2''(T, p'', x_2''). \qquad (14)$$

As the liquid and gas phases are considered ideal systems from assumption (3), equations (13) and (14) may be expressed as follows:

$$p_1' = x_1'' p_\infty \exp\left[\frac{v_L''(p'' - p_\infty)}{RT}\right] \qquad (15)$$

$$x_2'' = K p_2' \qquad (16)$$

where

$$1/K = \exp\left[\frac{\mu_2^0(T, p'') - \mu_2^{\ddagger}(T)}{RT}\right].$$

As the change of p'' is not big, K is considered to be constant, and Henry's law is applicable. Substituting equations (12)–(16) into the condition of equation (10), the following equation is obtained.

$$p''' - p_1' = -\frac{2\sigma}{r} - \frac{2\sigma_{gL}}{r_{gL}} + \frac{n_{20}}{(n_1'' + n_2'')K + (4\pi/3RT)r^3}. \quad (17)$$

Equation (17) gives the relation between outside pressure p''' and the radius of bubble r when the droplet system is in equilibrium condition. In Fig. 5, the relation between the outside pressure given by the above relation and the radius of bubble in the droplet system is indicated.
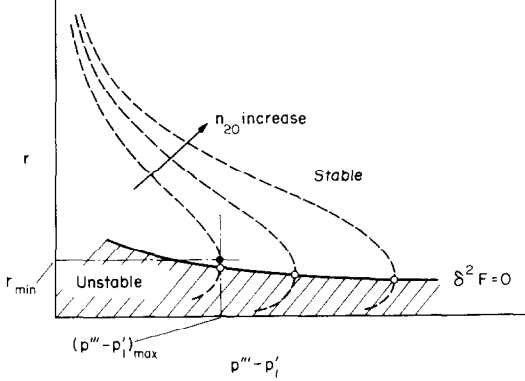

FIG. 5. Relation among r_{min}, $(p''' - p_1')_{max}$, and $\delta^2 F = 0$.

With the increase of outside pressure, the diameter of bubble in the droplet system decreases, and the maximum pressure is reached when the bubble radius is r_{min}. When the bubble radius is smaller than r_{min}, the bubble radius decreases with the outside pressure decreasing. Therefore, the bubble disappears at the pressure above $(p''' - p_1')_{max}$ in Fig. 5. For the bubble with radius smaller than r_{min}, the radius decreases with the pressure, and, physically speaking, such a state would not be considered to be realized. A close investigation of this is made in the following.

In general, ΔF, the difference of free energy F between two states where continuous changes occur in a solitary system, is expressed as follows, if Taylor's expansion is applied.

$$\Delta F = \delta F + \frac{1}{2!}\delta^2 F + \frac{1}{3!}\delta^3 F + \dots \quad (18)$$

As $\delta F = 0$ at the equilibrium point, when its second derivative is positive, it means the system is in a stable equilibrium condition. On the contrary, when the second derivative is negative, it means the system is in an unstable equilibrium condition. Changes of free energy of the system are equal to the work $-p'''\delta V_{gL}$ received from outside (the surrounding liquid). However, the volume change δV_{gL} of the droplet system and the outside pressure p''' are independent. Therefore,

$$(\delta p'''/\delta V_{gL})_{T, n_1', n_2'} = 0.$$

Consequently, the second derivative $\delta^2 F$ of free energy of this system is equal to the second derivative $\delta^2 F$ of free energy defined by equation (2), and the following equation is made.

$$\delta^2 F = \delta^2 F = \delta^2 F' + \delta^2 F'' + \delta^2 F^\sigma + \delta^2 F^{gL}. \quad (19)$$

Differentiating equations (4)–(7) and using equations (8)–(11), equation (19) is expressed as follows:

$$\delta^2 F = \left(\frac{\delta^2 F}{\delta V'^2}\right)_{n_1' n_2'} (\delta V')^2 + 2\left(\frac{\partial^2 F}{\partial V' \partial n_1'}\right)_{n_2'} (\delta V')(\delta n_1')$$
$$+ \left(\frac{\partial^2 F}{\partial V' \partial n_2'}\right)_{n_1'} (\delta V')(\delta n_2') + 2\left(\frac{\partial^2 F}{\partial n_1' \partial n_2'}\right)_{V'}$$
$$\times (\delta n_1')(\delta n_2') + \left(\frac{\partial^2 F}{\partial n_1'^2}\right)_{n_2' V'} (\delta n_1')^2$$
$$+ \left(\frac{\partial^2 F}{\partial n_2'^2}\right)_{n_1' V'} (\delta n_2')^2. \quad (20)$$

By making use of the above mentioned calculations, second derivatives are expressed as follows:

$$\left(\frac{\partial^2 F}{\partial V'^2}\right)_{n_1' n_2'} = \left\{\frac{\partial}{\partial V'}\left(\frac{2\sigma}{r} + \frac{2\sigma_{gL}}{r_{gL}} - p'\right)\right\}_{n_1' n_2'} \quad (21)$$

$$\left(\frac{\partial^2 F}{\partial n_1'^2}\right)_{V' n_2'} = \left[\frac{\partial}{\partial n_1'}\{\mu_1'(T, p_1') - \mu_1''(T, p'', x_1'')\}\right]_{V' n_2'} \quad (22)$$

$$\left(\frac{\partial^2 F}{\partial n_1'^2}\right)_{V' n_1'} = \left[\frac{\partial}{\partial n_2'}\{\mu_2'(T, p_2') - \mu_2''(T, p'', x_2'')\}\right]_{V' n_1'} \quad (23)$$

$$\left(\frac{\partial^2 F}{\partial V' \partial n_1'}\right)_{n_2'} = -\left(\frac{\partial p'}{\partial n_1'}\right)_{n_2'} \quad (24)$$

$$\left(\frac{\partial^2 F}{\partial V' \partial n_2'}\right)_{n_1'} = -\left(\frac{\partial p'}{\partial n_2'}\right)_{n_1'} \quad (25)$$

$$\left(\frac{\partial^2 F}{\partial n_1' \partial n_2'}\right)_{V'} = \left[\frac{\partial}{\partial n_2'}\{\mu_1'(T, p_1') - \mu_1''(T, p'', x_1'')\}\right]_{V' n_1'}. \quad (26)$$

Considering the above mentioned assumptions, the right terms of equations (21)–(26) are calculated by using thermodynamical formulae. Using assumption (4) of constant liquid phase volume and assumption (3), the r.h.s. of equation (21) is calculated as follows:

$$\left(\frac{\partial^2 F}{\partial V'^2}\right)_{n_1' n_2'} = -\frac{2\sigma}{4\pi r^4} - \frac{2\sigma_{gL}}{4\pi r_{gL}^4} + \frac{p'}{V'}. \quad (27)$$

As the liquid phase of the droplet system is also assumed ideal according to assumption (3), the derivative of the chemical potential of the first component of the liquid phase with respect to n_1' is given as

$$\left\{\frac{\partial\mu_1''(T, p'', x_1'')}{\partial n_1''}\right\}_{V'' n_2''} = \left\{\frac{\partial\mu_1^0(T, p'')}{\partial n_1''}\right\}_{V'' n_2''} + \frac{RT}{x_1''}\left(\frac{\partial x_1''}{\partial n_1''}\right)_{V'' n_2''} \quad (28)$$

where μ^0 is a standard chemical potential.

The following equation is obtained if the first term in the r.h.s. of equation (28) is expressed with the definition of compressibility.

$$\left\{\frac{\partial\mu_1^0(T, p'')}{\partial n_1''}\right\}_{V'' n_2''} = \left\{\frac{\partial\mu_1^0(T, p'')}{\partial p''}\right\}_{V''}\left(\frac{\partial p''}{\partial v''}\right)_{n_2''}\left(\frac{\partial v''}{\partial n_1''}\right)_{V'' n_2''}$$
$$= v_{10}'' \frac{1}{\kappa(n_1'' + n_2'')} \quad (29)$$

where,

$$v_{10}'' = \left\{\frac{\partial\mu_1^0(T, p'')}{\partial p''}\right\}_{V''}$$

expresses the specific volume of the liquid phase for $x_1'' \to 1$.

In the same way, by changing suffix 1 of equations (28) and (29) with suffix 2, a partial derivative of chemical potential of the second component of the liquid phase with respect to n_2'' is obtained. The r.h.s. of equations (22) and (23) are calculated by using the above mentioned formula which are respectively expressed as the following equations (30) and (31).

$$\left(\frac{\partial^2 F}{\partial n_1''^2}\right)_{V'n_2'} = \frac{RT}{n_1'} + \frac{v_{10}''}{\kappa}\frac{1}{(n_1''+n_2'')} + \frac{RT}{x_1''}\frac{x_2''}{(n_1''+n_2'')} \quad (30)$$

$$\left(\frac{\partial^2 F}{\partial n_2''^2}\right)_{V_1 n'} = \frac{RT}{n_2'} + \frac{v_{20}''}{\kappa}\frac{1}{(n_1''+n_2'')} + \frac{TR}{x_2''}\frac{x_1''}{(n_1''+n_2'')}. \quad (31)$$

Equations (24)–(26) are expressed as the following equations (32)–(34) by the similar calculation.

$$\left(\frac{\partial^2 F}{\partial V'\partial n_1'}\right)_{n_2'} = -\frac{RT}{V'} \quad (32)$$

$$\left(\frac{\partial^2 F}{\partial V'\partial n_2'}\right)_{n_1'} = -\frac{RT}{V'} \quad (33)$$

$$\left(\frac{\partial^2 F}{\partial n_1'\partial n_2'}\right)_{V'} = -\frac{RT}{(n_1''+n_2'')} + \frac{v_{20}''}{\kappa}\frac{1}{(n_1''+n_2'')}. \quad (34)$$

By making use of these equations, each term of the r.h.s. of equation (20) can be evaluated, and the sign of $\delta^2 F$ will be investigated. The quadratic formula of equation (20) is given as follows:

$$\delta^2 F = \lambda_1(\delta V^*)^2 + \lambda_2(\delta n_1^*)^2 + \lambda_3(\delta n_2^*)^2 \quad (35)$$

where $\lambda_1, \lambda_2, \lambda_3$ are eigenvalues of the following matrix:

$$\begin{vmatrix} \left(\frac{\partial^2 F}{\partial V'^2}\right)_{n_1'n_2'} & \left(\frac{\partial^2 F}{\partial V'\partial n_1'}\right)_{n_2'} & \left(\frac{\partial^2 F}{\partial V'\partial n_2'}\right)_{n_1'} \\ \left(\frac{\partial^2 F}{\partial n_1'\partial V'}\right)_{n_2'} & \left(\frac{\partial^2 F}{\partial n_1'^2}\right)_{V'n_2'} & \left(\frac{\partial^2 F}{\partial n_1'\partial n_2'}\right)_{V'} \\ \left(\frac{\partial^2 F}{\partial n_2'\partial V'}\right)_{n_1'} & \left(\frac{\partial^2 F}{\partial n_2'\partial n_1'}\right)_{V'} & \left(\frac{\partial^2 F}{\partial n_2'^2}\right)_{V'n_1'} \end{vmatrix}. \quad (36)$$

If the eigenvalues of the matrix of equations (36) are all positive, the second derivative of free energy of the system becomes positive and its equilibrium state can be said to be stable.

The necessary and sufficient condition for the matrix in equations (36) to be definite and positive is given by the following equations.

$$\left(\frac{\partial^2 F}{\partial V'^2}\right)_{n_1'n_2'} > 0 \quad (37)$$

$$\begin{vmatrix} \left(\frac{\partial^2 F}{\partial V'^2}\right)_{n_1'n_2'} & \left(\frac{\partial^2 F}{\partial V'\partial n_1'}\right)_{n_2'} \\ \left(\frac{\partial^2 F}{\partial n_1'\partial V'}\right)_{n_2'} & \left(\frac{\partial^2 F}{\partial n_1'^2}\right)_{V'n_2'} \end{vmatrix} > 0 \quad (38)$$

$$\begin{vmatrix} \left(\frac{\partial^2 F}{\partial V'^2}\right)_{n_1'n_2'} & \left(\frac{\partial^2 F}{\partial V'\partial n_1'}\right)_{n_2'} & \left(\frac{\partial^2 F}{\partial V'\partial n_2'}\right)_{n_1'} \\ \left(\frac{\partial^2 F}{\partial n_1'\partial V'}\right)_{n_2'} & \left(\frac{\partial^2 F}{\partial n_1'^2}\right)_{V'n_2'} & \left(\frac{\partial^2 F}{\partial n_1'\partial n_2'}\right)_{V'} \\ \left(\frac{\partial^2 F}{\partial n_2'\partial V'}\right)_{n_1'} & \left(\frac{\partial^2 F}{\partial n_2'\partial n_1'}\right)_{V'} & \left(\frac{\partial^2 F}{\partial n_2'^2}\right)_{V'n_1'} \end{vmatrix} > 0. \quad (39)$$

By substituting physical properties of materials into equations (37)–(39), and calculating the values of these equations, the equilibrium line ($\delta F = 0$), that is, the solid line in Fig. 5, can be divided into a stable and an unstable region. The white circle is the point of $\delta^2 F = 0$. The bubble bigger than this is stable ($\delta^2 F > 0$), and the one smaller unstable ($\delta^2 F < 0$). That is, the second derivative of free energy of the system changes its sign in the neighborhood of the radius r_{min} of the bubble corresponding to the maximum pressure in Fig. 5.

4. RESULT OF NUMERICAL CALCULATION

In order to satisfy assumptions (1)–(6), H_e, N_2, O_2, CO_2 gases are used in considering a small droplet of freon 21 floating in glycerine, and the result of numerical calculation is shown by using equation (17) and equations (37)–(39) concerning the relations among the outside pressure p''', the bubble radius r and the condition of changing sign of $\delta^2 F$. The physical properties of glycerine and freon 21 are shown in Table 1. Table 2 shows solubility of gas in freon 21 estimated by Hildebrand's method [8]. Taking comparison with experiment into account, calculation was made for

Table 1. Physical properties of liquid used

Liquid	Boiling point (°C)	(N₂) Solubility coefficient (at 25°C) (1/Pa)	(N₂) Diffusion coefficient (at 20°C) (m/s)	Viscosity coefficient (at 20°C) (Pa·s)	Surface tension (at 20°C) (N/m)
Freon-21	8.92	0.732×10^{-8}	4.11×10^{-9}	3.53×10^{-4}	18.0×10^{-3}
Glycerine	290	2.53×10^{-11}	9.75×10^{-13}	1.49	63.4×10^{-3}

Table 2. Solubility of gases in Freon-21 estimated from Hildebrand's method

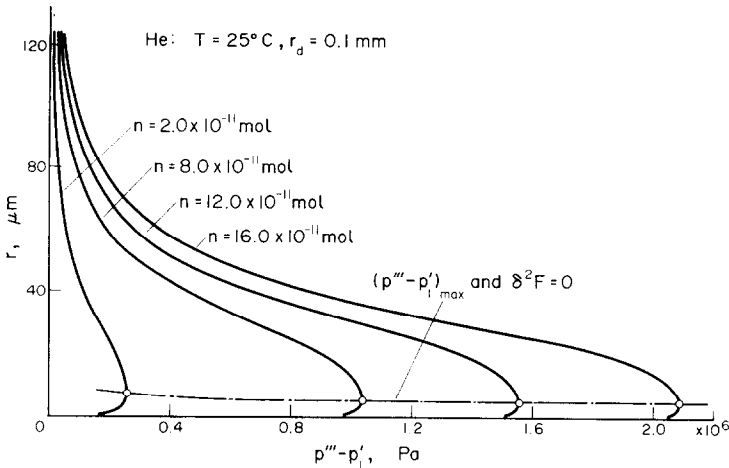| K	Gas			
	H_e	N_2	O_2	CO_2
Solubility coefficient (at 25°C) 1/Pa	1.36×10^{-9}	7.32×10^{-9}	1.97×10^{-8}	7.85×10^{-8}

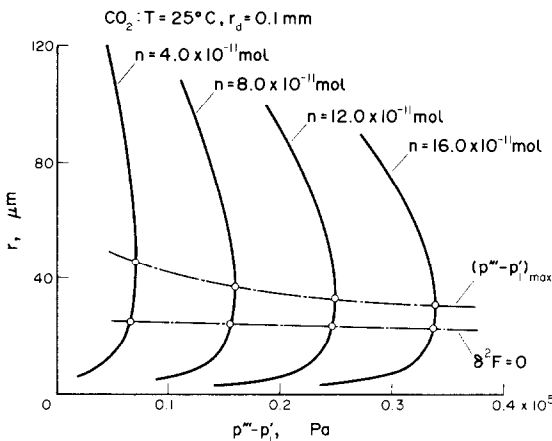FIG. 6. $p - r$ Relation of helium (theory).

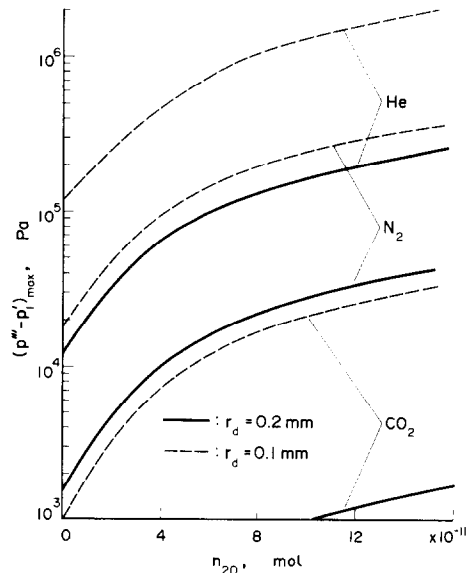FIG. 7. $p - r$ Relation of carbon dioxide (theory).

FIG. 8. Relation between mole number of noncondensable
gas and maximum pressure.

system temperature of $25°$, $r_2 = 0.1$ mm, 0.2 mm. In
Figs. 6 and 7, equation (17) of the bubble radius r and
$(p''' - p'_1)$, the difference between the outside pressure p'''
and the vapor pressure p'_1 of component 1 in the bubble
for H_e and CO_2 as dissolved gas, are shown by the solid
lines, and the points where $\delta^2 F$ becomes zero are
indicated. The curve $(p''' - p')_{max}$ in the figures shows the
maximum pressure that the system can reach under an
equilibrium condition. The curve of $\delta^2 F = 0$ in the
figures divides the region into the thermodynamically
stable region and unstable one. In the region above the
curve of $\delta^2 F = 0$, $\delta^2 F > 0$, while in the region below it
$\delta^2 F < 0$. As the result of numerical calculation, the
curve of $(p''' - p')_{max}$, which shows the limit of dynamical
stability, almost agrees with the limit of the thermal
stability given by $\delta^2 F = 0$ in the case of gas of low
solubility. However, in the case of CO_2 gas, which has
a high solubility, there exists a considerable difference
between the bubble radius for $(p''' - p')_{max}$, and $\delta^2 F = 0$.
The reason for this is considered to be the applicability
of Henry's law to such a soluble gas as CO_2 gas.
Therefore, it cannot simply be concluded that the
critical bubble diameter for $\delta^2 F = 0$ agrees in general
with that for $(p''' - p')_{max}$, and this problem is left for
further investigations. Figure 8 shows the relation
between the mol number of noncondensable gas and the

maximum pressure $(p''' - p')_{max}$, for the bubble radii of
$r_d = 0.1$ mm and 0.2 mm. The maximum pressure in-
creases with increase of mol number. For a given mol
number of noncondensable gas, the lower the solubility
of the gas is, such as CO_2, N_2 H_e, the higher the
maximum pressure is. From this figure the amount of
noncondensable gas contained in the droplet system can
be obtained when the maximum pressure $(p''' - p'_1)_{max}$ is
known. The result from another calculation shows that
with increase of the droplet radius r_d, the critical bubble
radius r_c in the system increases rapidly. Therefore,
at the extreme of $r_d \rightarrow \infty$, $r_c \rightarrow \infty$, the bubble of a
limited size existing in a sufficiently large liquid is in an
unstable condition.

Figure 9 shows the phenomenon investigated in this
paper schematically and from thermodynamical stand-
point. The equilibrium point 4 in the figure is the point
of $\delta^2 F = 0$. For the bubble whose radius is larger than
this $(1_a, 1_b)$ $\delta^2 F > 0$, and in the neighborhood of this
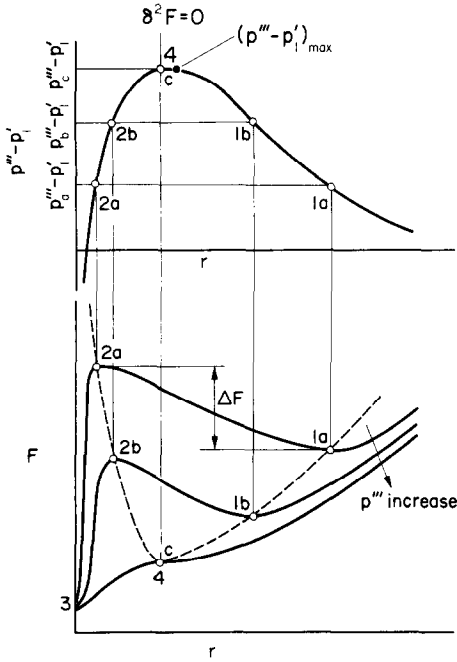point, the curvature surface of free energy is concave.

FIG. 9. Thermodynamic relation of bubble extinction.

On the other hand, when the bubble radius is smaller $(2_a, 2_b) \delta^2 F < 0$, and the cross-section in the r direction of the curve of free energy has a convex curve. The curvature surface of free energy near the equilibrium point 4 has a curvature surface like a bucket seat. Therefore, the bubble at this equilibrium point $(\delta^2 F = 0)$ disappears if disturbance is given. Now, when the outside pressure p''' is gradually raised from p_a''' to p_c''', the free energy F_{1a} at the stable equilibrium point 1_a falls down to F_{1b} and F_{1c}. At the same time, the free energy F_{2a} at the unstable point also falls down to F_{2b} and F_{2c}. Finally, at the point of $\delta^2 F = 0$, F_{1c} and F_{2c} become equal, and following the path of $1_a \rightarrow 1_b \rightarrow 1_c \rightarrow 4$ the bubble extinguishes. We call the pressure of bubble extinction as bubble extinction pressure. The bubble at 1 exists stably until it becomes a bubble of the radius at 4. The difference of free energies at 2_a and 1_a is the potential barrier for the bubble, and its energy rapidly decreases as it goes from p_a''' to p_c''' and becomes zero at 4. The bubble existing in the droplet is a bubble of radius above r_4.

5. EXPERIMENTAL RESULT AND CONSIDERATION

Experiment was made on the following three non-condensable gases with different solubility, N_2, O_2 and CO_2. The radius of the bubble tested was between 0.1–0.2 mm. The experimental temperature was 20–30°C, the amount of noncondensable gas contained in the droplet system was 1000–4000 ppm for N_2 and O_2, 4000–40000 ppm for CO_2. For the amount of non-condensable gas to this extent, the bubble extinction pressure was 3–6 atm. In comparing the experiment with the theory, each experiment condition was varied for each test, and, especially, the difference of droplet radius gave a big effect to the results. The bubble radius was made nondimensional by the droplet radius

after bubble extinction, and the pressure $p''' - p_1'$ was made nondimensional by the surface pressure σ/r_d. Then equation (17) is given as following using nondimensional values.

$$P = -\frac{2}{r} - \frac{2\left(\frac{\sigma_{gL}}{\sigma}\right)}{(1+r^3)^{1/3}} + \frac{\left(\frac{n_{20}}{n_f} \frac{r_d}{\sigma K}\right)}{1 + \left(\frac{v_L''}{KRT}\right)r^3} \quad (40)$$

where

$$P = \frac{p''' - p_1'}{(\sigma/r_d)} \quad (41)$$

$$r = \frac{r}{r_d}. \quad (42)$$

The results for O_2 and N_2 are shown in Figs. 10 and 11. The black circles and the white circles are experimental values, while the triangle mark indicates the minimum bubble radius that the experiment could reach. The pressure measured when a droplet extinguished is shown with vertical broken lines. The solid line in the figure is the corresponding theoretical curve given by equation (40), the square mark showing the pressure obtained theoretically for bubble extinction. The theoretical curve and the experimental result show a good agreement in a wide pressure region. The solubility used in the analysis was obtained from the correlation curve of the measured values. Measurement
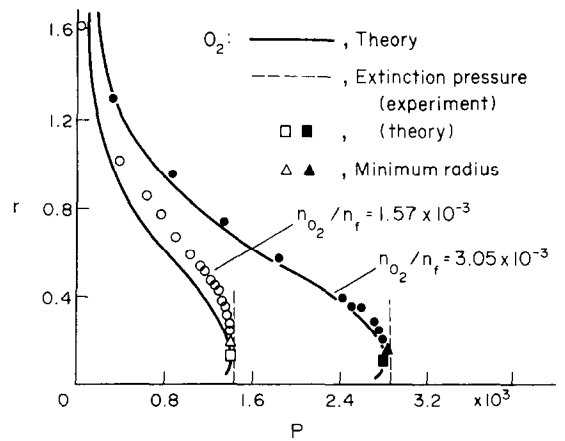
FIG. 10. $p - r$ Relation of oxygen (experiment).
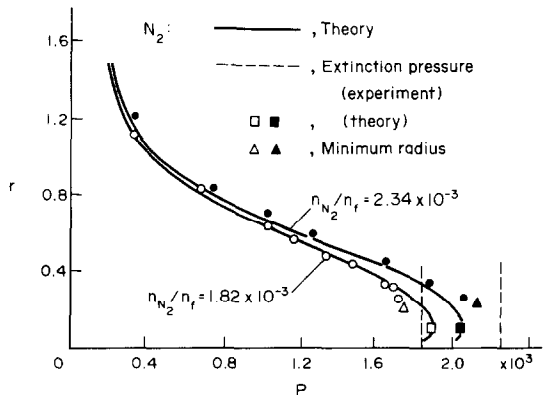
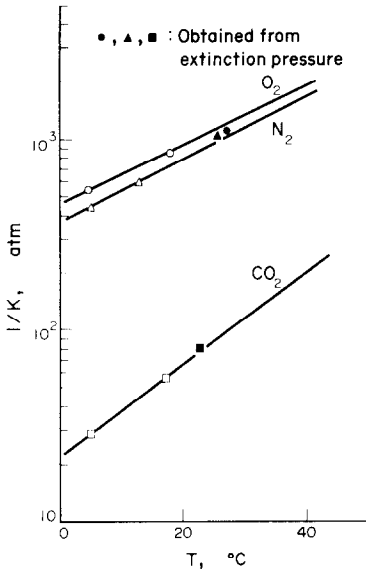FIG. 11. $p - r$ Relation of nitrogen (experiment).

FIG. 12. $T - 1/K$ Relation of various gases.

FIG. 13. $p - r$ Relation of carbon dioxide.

of solubility was made by the experimental apparatus described in Appendix 1; the result is shown with white marks in Fig. 12, the solid lines being the correlation lines and the black marks those in the analysis.

The result when a very small amount (1–4%) of CO_2 gas was added as noncondensable gas is shown in Fig. 13. The solid line is the theoretical line. As can be seen in the figure, there is a big difference between the theoretical curve and the measured value. This is because as CO_2 gas is very soluble the phenomenon may be greatly effected even by the existence of a small amount of less soluble gas such as air. Therefore, we shall now examine what effect the mixing of air will give to the relation of nondimensional pressure P and nondimensional radius r. If a mixture gas of CO_2 and air is considered for noncondensable gas, equation (40) is reduced as

$$p''' - p_1' = -\frac{2\sigma}{r} - \frac{2\sigma_{gL}}{r_{gL}}$$
$$+ \frac{n_{CO_{20}}}{(n_1'' + n_{CO_2}'' + n_{air}'')K_{CO_2} + (4\pi/3RT)r^3}$$
$$+ \frac{n_{air_0}}{(n_1'' + n_{CO_2}'' + n_{air}'')K_{air} + (4\pi/3RT)r^3}. \quad (43)$$

Here, n_{air_0} is the mole number of air contained in the droplet system. As the solubility of N_2 and O_2 is almost the same, the value of solubility coefficient for air in freon 21 was obtained by using the mole average calculated from measured values. In the experiment using CO_2 as noncondensable gas, as a result of measurement of components, under the experimental condition of white circle marks in Fig. 13, 450 ppm air was mixed, while under the experimental condition of black circle marks 503 ppm air was mixed in. Taking this air quantity into consideration, calculation was made with equation (7), shown in Fig. 13, since the theoretical curve and the experimental value show a good agreement. Therefore, between the theoretical
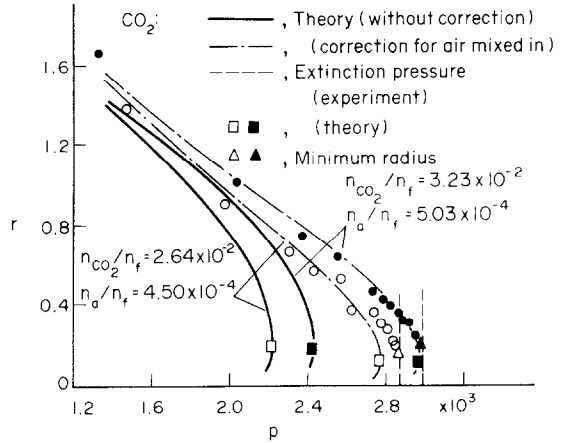
curve (solid line) without adjustment of air mixing and the experimental value is due to a very small amount of mixed air. That is, for soluble CO_2, even when a few % of air is mixed the air will not dissolve when the pressure is raised, while CO_2 almost dissolves and the bubble is occupied mostly by the air. Therefore, air gives a big effect when the bubble radius is small. The solubility of CO_2 used in the calculation is shown with the black square in Fig. 12.

From the result mentioned above, the relation between the mole number of noncondensable gas in the droplet system and the bubble extinction pressure is obtained and is shown in Fig. 14. In the figure, P_e, the nondimensional extinction pressure, is taken along the horizontal axis, and n_{20}/n_1, the mole fraction of noncondensable gas along the vertical axis. The solid line is the theoretical curve calculated by using the actually measured value of solubility coefficient. It is known from this figure that the theoretical curve and the
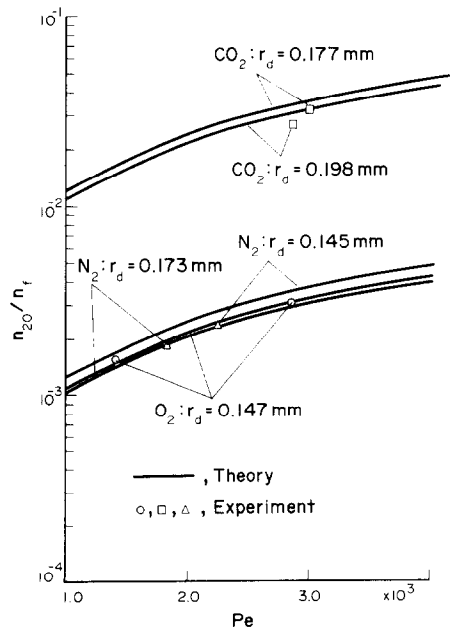

FIG. 14. Relation between extinction pressure and mole number of noncondensable gas.

experimental value show a good agreement. As the result, the volume of noncondensable gas contained in the droplet system can be known from the bubble extinction pressure, and contrarily, based on the volume of noncondensable gas, its solubility can be obtained.

6. CONCLUSION

As a fundamental step for the study of extinction and generation of bubble nucleus in boiling and cavitation, a thermodynamic analysis was made on behaviors of small gas bubble in the droplet system, and an experimental study was made on behaviors of gas bubble by making use of the droplet system containing gas bubble. The following conclusions are obtained.

(1) The small gas bubble in the droplet, whose diameter decreases with the rise of pressure, extinguishes when it reaches a certain critical pressure at a certain finite bubble diameter: it has been made clear that there holds a fairly good agreement between the theoretical prediction and experimental results with regard to the critical extinction pressure and bubble radius.

(2) When the droplet diameter and the volume of noncondensable gas are given, it is proved theoretically and experimentally that the bubble of diameter smaller than the critical value (the diameter at $\delta^2 F = 0$) cannot exist in the droplet.

(3) When a coefficient of gas disolution is given, the gas volume dissolved in the droplet can be calculated by extinction pressure of bubble. Also, when the volume of noncondensable gas contained in the droplet system is given, the coefficient of gas dissolution can be obtained by extinction pressure of bubble. Those results are made clear by comparing the theoretical result with the experimental result.

REFERENCES

1. H. Wakeshima and K. Takata, On the limit of superheat, *J. Phys. Soc. Japan* **13**, 1398 (1958).
2. W. Döring, Die Überhitzungsgrenze und Zerreissfestigkeit von Flussigkeiten, *Z. Phys. Chem.* **36**, 371 (1937).
3. V. P. Skripov and E. N. Sinitsyn, Kinetics of nucleation in superheated liquids, *Russ. J. Phys. Chem.* **42**, 440 (1968).
4. J. Frenkel, *Kinetic Theory of Liquids*. Dover, New York (1955).
5. H. K. Fauske, On the mechanism of uranium dioxide–sodium explosive interactions, *Nucl. Sci. Engng* **51**, 95 (1973).
6. M. Blander, D. Hengstenberg and J. L. Katz, Bubble nucleation in *n*-pentane, *n*-hexane, *n*-pentan + hexadecane, *J. Phys. Chem.* **75**, 3613 (1971).
7. J. S. Rowlinson, *Liquid and Liquid Mixtures*. Butterworth, London (1969).
8. J. H. Hildebrand and J. E. Jolley, Solubility, entropy and partial molal volumes in solutions of gases in nonpolar solvents, *J. Am. Chem. Soc.* **80**, 1050 (1958).
9. J. H. Perry, *Chemical Engineers' Handbook*. McGraw-Hill, New York (1963).
10. G. Houghton, A. M. Mclean and P. D. Ritchie, Compressibility, fugacity and water-solubility of carbon dioxide in the region 0–36 atm and 0–100°C, *Chem. Engng Sci.* **6**, 132 (1957).

APPENDIX

Measurement of Gas Dissolubility

Measurement of gas dissolubility of N_2, O_2, CO_2 in freon 21 was carried out in the following procedure. The measurement section consists of a pirex glass pipe of 6 mm I.D. and 1 m in length connected with a glass–teflon needle valve combined on the one end and on the other end with a U-tube of about 3 m length and a reservoir filled with mercury. The upper part of the glass pipe of the measurement section and the teflon needle valve are surrounded by water (+ ice) for keeping it warm.

By decreasing the mercury reservoir pressure, the test section is sufficiently degassed. The mercury reservoir is then raised, and the whole part of the test section is filled with mercury. When the needle valve is closed, about 8 cm³ (1.5–2 atm) gas is introduced into the test section, and the gas volume and pressure are measured from the height of the mercury. The gas filled in the pipe path to the inlet of the needle valve is exhausted. Then freon 21 vapor (about 2–3 atm) is introduced to the inlet of the needle valve of the test section. As the temperature of the test section is low, the freon 21 vapor is condensed and becomes liquid near and around the inlet of the needle valve. Four cm³ of freon 21 liquid is injected into the test section. After liquid freon 21 and noncondensable gas are introduced, the mercury reservoir is raised by shaking it up and down to increase pressure. The mercury reservoir is shaken up and down occasionally to oscillate the liquid freon 21 and to promote the gas being dissolved and diffused in the liquid. After a sufficient time is given for the freon 21 liquid and the gas to reach an equilibrium state, measurements are made on the gas volume and pressure. Considering the gas to be ideal, the gas volume dissolved into the liquid was calculated, and the dissolubility coefficient was obtained by Henry's law. In order to check the accuracy of the dissolubility measured, the dissolubility of CO_2 gas in water was measured. The measured value is $K = 1.07 \times 10^{-9}$ cm²/dyn ($T = 5°C$), and the actually measured values of Perry [9], Houghton [10] are 1.16×10^{-9}, 1.20×10^{-9} cm²/dyn, respectively. The results agree with our measured value within about 10% accuracy.

ETUDE FONDAMENTALE DE LA DISSOLUTION DES BULLES DANS UN LIQUIDE

Résumé—Constituant une étape fondamentale dans l'étude de la résorption et de la formation de bulles au cours de l'ébullition et de la cavitation, des travaux théoriques et expérimentaux ont été effectués sur le mode de résorption des bulles gazeuses en utilisant des gouttelettes contenant des bulles gazeuses. Une petite bulle gazeuse à l'intérieur de la gouttelette, dont le diamètre diminue lorsque la pression augmente, se résorbe lorsqu'une certaine pression critique est atteinte pour un certain diamètre fini de la bulle. Le phénomène est analysé du point de vue de l'instabilité thermodynamique en considérant la dissolution d'un gaz dans un liquide. On montre que les prévisions théoriques et les résultats expérimentaux présentent un très bon accord en ce qui concerne la pression critique et le rayon de la bulle.

Y. Mori, K. Hijikata and T. Nagatani

GRUNDLEGENDE UNTERSUCHUNG DER AUFLÖSUNG VON BLASEN IN FLÜSSIGKEITEN

Zusammenfassung—Als grundlegender Schritt beim Studium des Zerfalls und der Bildung von Blasenkeimen bei Siede- und Kavitationsvorgängen wurde eine theoretische und experimentelle Untersuchung des Zerfallsverhaltens von Gasblasen durchgeführt; dabei fand das gasblasenenthaltende Tröpfchensystem Verwendung. Eine kleine Gasblase in einem Tröpfchen, dessen Durchmesser mit zunehmendem Druck abnimmt, zerfällt nach den Versuchen, wenn ein bestimmter kritischer Druck und ein bestimmter endlicher Blasendurchmesser erreicht ist. Das Phänomen wird unter Betrachtung der Auflösung von Gasen in Flüssigkeiten über eine thermodynamische Instabilität gedeutet. Es wird gezeigt, daß zwischen den theoretischen Vorhersagen und den experimentellen Ergebnissen in bezug auf den kritischen Druck und den Blasenradius eine recht gute Übereinstimmung besteht.

ФУНДАМЕНТАЛЬНОЕ ИССЛЕДОВАНИЕ РАСТВОРЕНИЯ ПУЗЫРЬКА В ЖИДКОСТИ

Аннотация — Выполнено теоретическое и экспериментальное изучение исчезновения и образования пузырьков газа при кипении и кавитации с помощью капельной системы, содержащей пузырек газа. При определенном критическом давлении и конечном диаметре пузырька пузырек газа в капле, диаметр которой уменьшается с увеличением давления, исчезает. Это явление анализируется с точки зрения термодинамической нейстойчивости с учетом растворимости газа в жидкости. Показано, что наблюдается достаточно хорошее соответствие между теоретическим расчетом и экспериментальными данными в отношении критического давления и радиуса пузырька.